J. Mol. Biol. (1997) **268**, 412–423

JMB

Apoprotein Structure in the LH2 Complex from *Rhodopseudomonas acidophila* Strain 10050: Modular Assembly and Protein Pigment Interactions

S. M. Prince[1], M. Z. Papiz[3], A. A. Freer[1], G. McDermott[1] A. M. Hawthornthwaite-Lawless[3], R. J. Cogdell[2] and N. W. Isaacs[1]*

[1]*Department of Chemistry*
[2]*Division of Biochemistry and Molecular Biology, University of Glasgow, Glasgow, G12 8QQ UK*

[3]*CCLRC Daresbury Laboratory Daresbury, Warrington WA4 4AD, UK*

**Corresponding author*

The refined structure of the peripheral light-harvesting complex from *Rhodopseudomonas acidophila* strain 10050 reveals a membrane protein with protein-protein interactions in the trans-membrane region exclusively of a van der Waals nature. The dominant factors in the formation of the complex appear to be extramembranous hydrogen bonds (suggesting that each apoprotein must achieve a fold close to its final structure in order to oligomerize), protein-pigment and pigment-pigment interactions within the membrane-spanning region. The pigment molecules are known to play an important role in the formation of bacterial light-harvesters, and their extensive mediation of structural contacts within the membrane bears this out. Amino acid residues determining the secondary structure of the apoproteins influence the oligomeric state of the complex.

The assembly of the pigment array is governed by the apoproteins of LH2. The particular environment of each of the pigment molecules is, however, influenced directly by few protein contacts. These contacts produce functional effects that are not attributable to a single cause, e.g. the arrangement of an overlapping cycle of chromophores not only provides energy delocalisation and storage properties, but also has consequences for oligomer size, pigment distortion modes and pigment chemical environment, all of which modify the precise function of the complex. The evaluation of site energies for the pigment array requires the consideration of a number of effects, including heterogeneous pigment distortions, charge distributions in the local environment and mechanical interactions.

Keywords: light-harvesting; membrane protein; photosynthesis; pigment; X-ray structure

Introduction

The recently determined structure of the light-harvesting complex from the purple photosynthetic bacteria *Rhodopseudomonas acidophila* strain 10050 (McDermott *et al.*, 1995), has revealed a modular complex with pigment molecules enclosed by protein (Figure 1). Purple bacterial light-harvesting complexes modify the absorption properties of their chromophores to wavelengths such that the spectrum available to them *in vivo* is maximised; and the energy so absorbed is productively transferred and made available for photochemistry. The environment of the chromophores in the light-harvesting complex is governed by protein. The protein creates the conditions determining the relative disposition of the pigments, and contributes to the local environment that modulates their absorption spectra.

The initial photochemical redox reaction in purple bacteria takes place in the reaction centre complex (RC), where an absorbed photon leads to charge separation across the membrane (reviewed by Feher *et al.*, 1989). In order to increase the spectral cross-section of absorption, purple bacteria also produce light-harvesting complexes. In most

Abbreviations used: LH1/2, core/peripheral light-harvesting complex; Bchl *a*, bacteriochlorophyll *a*; B800 and B850, 800 and 850 nm absorbing bacteriochlorophyll *a*s; RC, reaction centre; PC, protomer complex; CD, circular dichroism; IR, infra red.

0022–2836/97/170412–12 $25.00/0/mb970966

Figure 1. A schematic of the LH2 molecule; the helices are represented by ribbons and the photoactive portion of the chromophores are shown. Below, a representation of the protomer complex; the complete pigments are included in a stick representation (MOLSCRIPT; Kraulis, 1991).

cases a primary light-harvesting complex (LH1) and peripheral light-harvesting complexes (LH2) are synthesised (Zuber & Brunisholz, 1991). LH1 complexes are found in stoichiometric equivalence with the RC, while LH2 complexes are produced in variable amounts according to the available light levels, the absorbance range of the particular LH2 (800 and 850, 800 and 820 nm), the temperature, and the bacterial species and strain (Zuber & Brunisholz, 1991).

When purple bacteria are grown under anaerobic conditions they incorporate the photosynthetic apparatus described above into invaginated intracytoplasmic phospholipid membranes. RC, LH1 and LH2 are integral trans-membrane assemblies. After absorption of a photon by a pigment molecule all energy transfer processes occur within the membrane until energy is ''trapped'' by the RC complex (van Grondelle *et al*., 1994). Here, we consider the influence of the apoproteins on the function and assembly of LH2. The detailed mechanisms of energy transfer within the LH2 complex are considered elsewhere (Freer *et al*., 1996; Sauer *et al*., 1996) and the mode in which RC, LH1 and LH2 might assemble to form a photosynthetic unit (Papiz *et al*., 1996) will not be considered here.

Each individual light-harvesting complex is composed of oligomers of short peptides (α and β) with associated pigments (Hawthornthwaite & Cogdell, 1991). αβ apoproteins with their non-covalently bound carotenoid and bacteriochlorophyll *a* (Bchl *a*) pigments form the multi-subunit complexes LH1 and LH2. Primary structure analysis of, individually, the α apoproteins of LH2, and the β apoproteins of LH2, across all species and strains of purple bacteria reveals a high degree of homology. This homology extends to a lesser extent to the α and β apoproteins of LH1 (Zuber, 1986). The differences between the LH1 and LH2 complexes reside in their protein/pigment stoichiometry and modes of oligomerization. Structural studies have shown that LH2 complexes are formed from eight or nine αβ subunit oligomers (McDermott *et al*., 1995; Koepke *et al*., 1996; Savage *et al*., 1996) whereas LH1 complexes comprise 16 subunits (Karrasch *et al*., 1995).

Results and Discussion

Apoprotein structure

The apoproteins from the PC of *Rps. acidophila* are shown in Figure 1. The C_9 molecular symmetry axis is presumed to be coincident with the membrane normal. The crystal structure of LH2 reveals all 41 residues of the β apoprotein, and residues 1 to 49 in the 53 residue α polypeptide; the remaining four C-terminal residues according to the published sequence (Zuber & Brunisholz, 1991) are Lys, Lys, Ala and Ala, and are not observed in the electron density maps. Table 1 details the secondary structure assignments derived by PROCHECK (Laskowski *et al*., 1993). Each apoprotein possesses a long trans-membrane α-helix (Table 1) which incorporates the hydrophobic membrane-spanning segments α(12-35), β(13-37).

In the β apoprotein the trans-membrane (8-9 turn) helix begins after a four-residue N-terminal extended section. The five C-terminal residues terminate in a short loop. The β apoprotein transmembrane helix is slightly curved and is inclined to the C_9 axis at an angle of approximately 15°. The membrane-spanning segment of the α apoprotein is, in the main, parallel with the C_9 axis. Proceeding from the N-terminal Met residue of α, a

Table 1. Secondary structure of apoproteins

Residues	Secondary structure assignment	Sequence
α1-α3	–	MNQ
α4-α8	3_{10} Helix	GKIWT
α9-α11	–	VVN
α12-α36	α Helix	PAIGIPA LLGSVTV IAILVHL AILS
α37-α39	–	HTT
α40-α46	α Helix	WFPAYWQ
α47-α49	–	GGV
α50-α53	[Disordered]	KKAA
β1-β4	–	ATLT
β5-β36	α Helix	AEQSEEL HKYVIDG TRVFLGL ALVAHFL AFSA
β37-β41	–	TPWLH

three-residue loop involved in the coordination and environ of a Bchl *a* molecule gives way to a short section of 3_{10} helix. The 3_{10} helix penetrates the plane of the membrane surface. A three-residue section links the 3_{10} helix to the trans-membrane helix, a seven-turn α-helix. This is followed by a three-residue section then a two-turn amphipathic helix. The C-terminal portion including the four ''missing'' residues begins with consecutive Gly residues, and appears to be mobile, extending away from the body of the complex.

Tertiary structure

The turns at the C and N termini of β are exposed to an aqueous environment. These turns are characterised by a side-chain to main-chain hydrogen bond involving hydrophilic residues. At the N-terminal end of the β trans-membrane helix an amphipathic extended stretch turns into a helix. This change of structure is stabilised by the interaction between βThr4 and βGlu7. βGlu7 is on the first turn of the helix and the side-chain oxygen atom accepts a hydrogen bond from the main-chain nitrogen atom of βThr4. This is matched by a hydrogen bond accepted by the OH group of βThr4 from the main-chain nitrogen atom of βGlu7. At the C-terminal end, the membrane-spanning helix is disrupted by βPro38. This leads to a loop with the N^{δ} of the terminal His residue donating a hydrogen bond to the main-chain carbonyl oxygen atom of βThr37. The intervening hydrophobic Trp and Leu residues at β39 and 40 dip back into the complex.

Turns in the α apoprotein have consequences for oligomerization and pigment binding. The N-terminal portion of α is involved in the binding of a Bchl *a* pigment, and is submerged in the membrane. The electron density of the LH2 crystal structure indicates a modified (formylated) N terminus (McDermott *et al.*, 1995), suggesting that a charged terminus is not buried. The N-terminal section of the β apoprotein extends beyond the trans-membrane stretch of the α apoprotein, partially covering the N-terminal 3_{10} helix and the turn between this and the membrane-spanning helix of α (Figure 1). This turn, comprising residues α9 to α11, takes the form of a long S. The turn is stabilised by steric interactions between αTrp7 and αPro12 at the end of the 3_{10} and beginning of the trans-membrane helices. The axis of the first two turns of the trans-membrane helix is not parallel with the C_9 axis. This is rectified by αPro17, which alters the helix direction making the remainder of the helix parallel with the C_9 axis. This helix distortion by αPro17 allows the N-terminal 3_{10} helix to pass to one side of the radially associated β trans-membrane helix, and may assist in the re-insertion into the membrane of the 3_{10} helix.

At the C-terminal end of the trans-membrane helix of α a loop leads to a short amphipathic helix, which is exposed to the cytoplasm. The formation of this helix is affected by αPro42, which prevents hydrogen bond formation and thus affects the angle at which the amphipathic helix lies with respect to the radius direction of the complete LH2 complex. Oligomerization contacts are made by this helix, both directly and *via* Bchl *a* contacts. Both C_9 and C_8 molecular symmetry occurs in LH2 complexes (McDermott *et al.*, 1995; Savage *et al.*, 1996; Koepke *et al.*, 1996), and a heptameric aggregate has been proposed for the *Rubrivax gelatinosus* LH2 (Jirsakova *et al.*, 1995). The local differences determining a 45° or even 51.4° rotational oligomer repeat as against one of 40° may be minor. In the octameric structure of *Rhodospirillum molischianum* the residue equivalent of αPro42 is tryptophan (Koepke *et al.*, 1996), and in *Rubrivax gelatinosus* it is glycine (Zuber & Brunisholz, 1991).

Membrane interaction

The LH2 complex forms a ring within the membrane and therefore encloses a volume of phospholipid. Electron density distributions within this region of the crystallographic structure are weak and difficult to interpret (Figure 2). It is known that LH2 purified in our studies contains lipid (G. Dahler & P. J. Dominy personal communication). At the boundary of this enclosed region (surrounded by the α apoproteins) C_9 symmetric distributions of low electron density are found. These structures are consistent with partial lipid molecules, although no lipid head group is observed. Although the radius of this region at 12 Å is of intermediate size with regard to protein secondary structure elements and could accommodate a single α-helix, gel electrophoresis gives no evidence of the presence of any additional protein. As the bounding α apoprotein trans-membrane helices present an hydrophobic enclosure (the most hydrophilic residue accessible is αSer24), no specific chemical interaction is likely between the contents of this volume and the LH2 complex. The structure of the LH2 from *Rh. molischianum* shows different electron density distributions, which have been in-

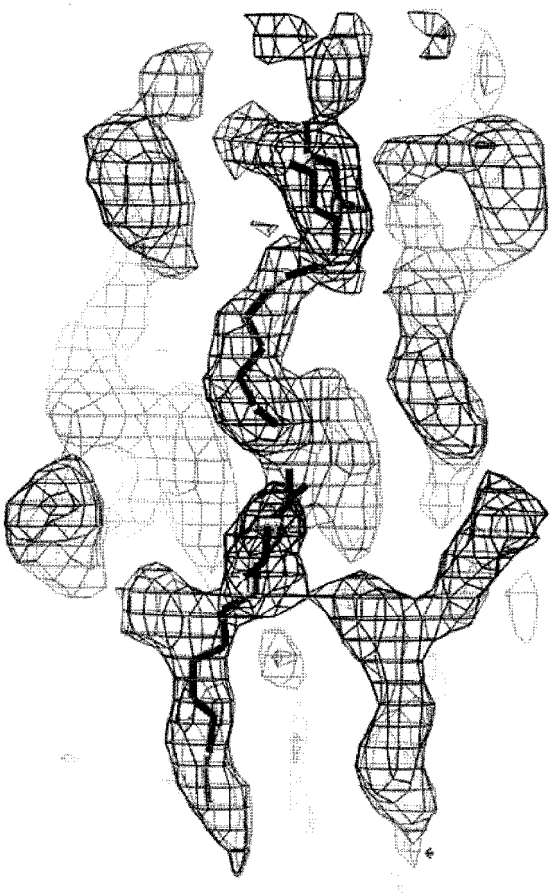

Figure 2. Electron density in the central ''hole'' of LH2. Averaged $F_o - F_c$, $2F_o - F_c$ and experimentally phased maps. A fit of β-octylglucoside detergent molecules is shown to give scale, although the density distributions are not satisfactorily accounted for with this detergent model (O; Jones *et al*., 1991).

terpreted as detergent and small amphiphile molecules (Koepke *et al*., 1996).

The external surface of LH2 is provided mainly by the inclined β apoproteins. Apart from the ion pair β17/20, this surface is very hydrophobic. Portions of B800 and B850 plus a putative second independent carotenoid (Freer *et al*., 1996) are exposed within the membrane-spanning region.

Other membrane proteins for which high-resolution structures exist have been shown to possess a band of hydrophobic aromatic residues protruding from the external surface of the structure at the level of membrane emergence (Cowan, 1993). These residues are thought to act as membrane anchors. No such arrangement is found in the LH2 structure. A number of factors may account for this. (1) The outer surface of LH2 is formed from both co-factor and protein, and as the molecular mass proportion of pigments is high, there is proportionally less protein-lipid interaction. (2) LH2 is a modular protein and membrane anchorage could obstruct the formation of LH2 or induce stress in the assembled complex. (3) LH2 must be in close physical contact with either LH1 or other LH2 complexes in order to function with the required efficiency (Kuhlbrandt, 1995). Consequently *in vivo* the immediate environment of the LH2 complex is both protein and lipid, and anchors may be obstructive to the close approach of LH2-LH2, and LH2-LH1.

Individual residues

Protein-protein interactions

The formation of the LH2 complex and therefore the relative dispositions of the pigments is strongly influenced by interactions amongst the pigments themselves. However, specific hydrogen-bonding contacts between the apoproteins of the complex can be located. These contacts precisely define the relative orientations of the subunits as reflected in the exactitude of the non-crystallographic symmetry encountered in the LH2 structure. The oligomerization contacts are found at the periplasmic and cytosolic facing ends of the LH2 complex. They predominantly involve side-chains (only one is of a β-sheet type interaction) and are relatively few in number (Table 2). Notable within these interactions is that of the side-chain of αTyr44, which forms a dual function in oligomer formation and in Bchl *a* coordination.

β Trans-membrane helices are isolated from each other, and so interact only with pigments. Within the trans-membrane region, protein-protein contacts are limited to hydrophobic interactions between adjacent α-apoprotein helices. The saturated phytyl chain of the αB850 molecule inserts between the adjacent helices, as does the saturated portion of the wholly defined carotenoid. These subdivide the direct protein-protein interactions into three regions (Figure 3). At the C-terminal end of LH2 the residues α_1Ile34, α_1Ala33 and α_2Leu35 form steric interactions with a ''key'' residue α_2Trp45, whose side-chain inserts between the two helices. In the central portion of the trans-membrane region a trimer of residues, α_2Thr24, α_1Ile26 and α_2Ile28, form close interactions, and towards the N termini a similar key arrangement is formed with α_1Gly15, α_2Ile16 and α_2Pro17, with α_1Val10 the inserting side-chain. αTrp45 the periplasmic key residue is also involved in B850 Bchl *a* coordination. Some of the residues involved in α-α contacts are also in-

Table 2. Strong oligomerizing H-bonds

Residue	Atom	Residue	Atom	Distance (Å)
Gly α4	O	Ser β8	OG	2.58
Trp α7	O	Leu β3	N	2.99
Thr α39	N	Gln (+)α46	OE1	2.65
Trp α40	NE1	Trp (+)α45	O	2.81
Tyr α44	OH	Trp (−)β39	NE1	3.22

The plus and minus symbols indicate proceeding/preceding PCs anticlockwise about the membrane normal.

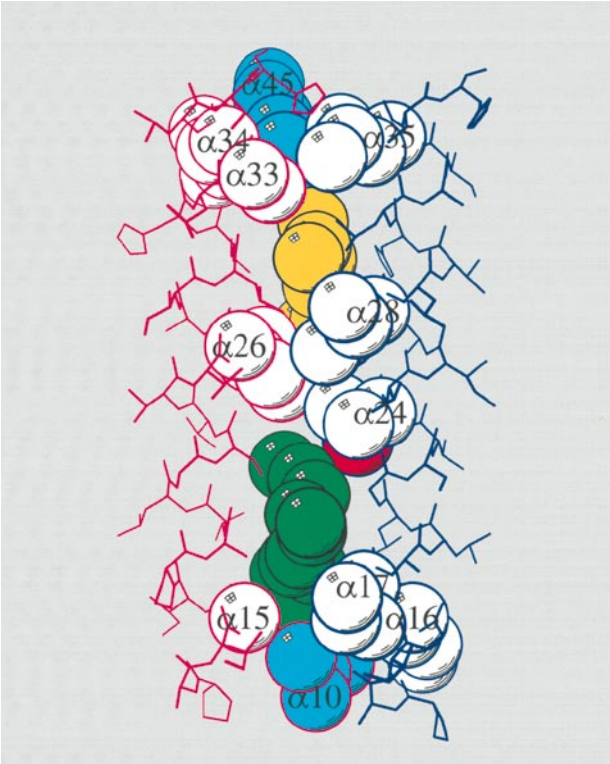

Figure 3. The α-α trans-membrane helix interaction. Pigments and interacting residue side-chains are shown as van der Waals spheres, atoms are coloured green for phytyl chain, yellow for carotenoid, ''key'' residues are cyan, remaining residues are coloured according to atom type; white C, red O (MOLSCRIPT; Kraulis, 1991).

volved in providing the environment of a pigment (Tables 3 to 6).

The lining of the presumed lipid-filled core is formed by hydrophobic residues along one face of each α polypeptide. The residue side-chains αIle14, Ala18, Gly21, Ser22, Val25, Leu29 and Leu32 of the trans-membrane helix face the lipid. This subset may vary independently within the constraint of hydrophobicity, and a sequence alignment of peripheral harvesters reveals a degree of variation amongst these residue species (Zuber & Brunizholz, 1991).

Pigment coordination

All Bchl *a* molecules in LH2 have two specific interactions with protein. The primary contact, the coordination of the magnesium central ion, is through a histidine residue (Robert & Lutz, 1985) for the B850 molecules and in the case of B800 is thought to be a coordination through the oxygen atom of a formylated αMet1. The other interaction is a hydrogen bond to the C3-acetyl group on ring A of Bchl *a*. The donor residues for this interaction are αTrp45 for αB850, αTyr44 (from the adjacent α protein) for βB850, and βArg20 for B800 (see Tables 3, 4 and 5). The keto group on ring E of any Bchl *a* molecule does not accept a hydrogen bond.

Table 3. Apoprotein contacts to the αB850 bacteriochlorin

αB850 atom	Residue	Atom	Distance (Å)
Mg	His α31	NE2	2.34
$O3^1$	Trp α45	NE1	2.97
C5	Phe α41	CZ	3.73
$C3^2$	Val (−)α30	CG1	4.36
$C7^1$	Tyr α44	CE2	4.00
$C8^1$	Trp α40	CH2	3.73
$C8^8$	Ile α34	CD1	3.98
$C12^1$	Ala β33	CB	4.14
C13	Ala β29	CB	3.43
$O13^1$	His β30	CE1	3.19
	Ala β26	CA	3.43
$C13^4$	Leu β25	CB	3.56
$O17^3$	Ala α27	CB	3.35
OP	Phe β22	CE1	3.34

The Bchl *a* numbering scheme used throughout is the IUPAC scheme outlined by Scheer (1991). Oxygen atoms are labelled according to the connecting carbon atom. Where carbonyl and ester type oxygen atoms are connected to the same carbon atom, the carbonyl takes precedence. i.e. in this Table $O17^3$ a carbonyl and OP an ester oxygen are connected to the same carbon atom immediately before the phytyl chain begins.

In the B850 cyclic overlapping ring, the N^{δ} of the opposing apoprotein histidine residue (that coordinating the other B850 within the PC) lies within hydrogen-bonding distance of this oxygen atom. However the angle of the O..H-N^{δ} bond is approximately 90°, suggesting only a small (if any) interaction. This gives rise to a possibility that, an N^{δ}-H..$O13^1$ interaction forms a transient structure in the formation of LH2. This might account for the high specificity of His for B850 coordination (Zuber, 1986).

The B850 molecules in LH2 are coordinated to their ligating apoproteins such that the phytyl chain is directed from the bacteriochlorin plane towards the trans-membrane helix (Figure 1) with the initial portion of the phytyl chain making steric interactions with the polypeptide. Extensive interactions between B850, B800 and carotenoid form a pigment ring enclosed by the apoproteins. This ring is penetrated only by βPhe22, which is highly

Table 4. Apoprotein contacts to the βB850 bacteriochlorin

βB850 atom	Residue	Atom	Distance (Å)
Mg	His β30	NE2	2.34
$O3^1$	Tyr (+)α44	OH	2.64
C10	Ile α34	CD1	3.63
C7	Trp β39	CE2	3.43
$C7^1$	Trp (+)α45	CD1	3.54
$C8^2$	Trp α40	CH2	3.98
	Thr β37	CG2	4.09
	Ala β33	CB	3.88
C12	Val α30	CG1	3.64
$C12^1$	His α31	CE1	3.41
$O13^1$	Ala α27	CB	3.51
$C13^4$	Val α23	O	3.72
	Ile α26	CG2	4.12
$O17^3$	Leu β23	CA	3.86
	Ala β26	CB	3.28
OP	Phe β22	CD2	3.48

Table 5. Apoprotein contacts to the B800 bacteriochlorin

B800 atom	Residue	Atom	Distance (Å)
Mg	fMet α1	OF	2.46
$O3^1$	Arg β20	NH2	2.91
C1	Ile β16	CD1	3.68
C10	Gln α3	NE2	3.83
$C2^1$	Thr β19	CG2	3.63
$C7^1$	Asn α2	OD1	3.47
$C12^1$	Gly (+)β18	CA	3.65
	Val (+)β21	CB	4.08
$O13^4$	Leu (+)α20	CD1	3.91

conserved in the β apoproteins of LH1 and LH2. This residue interacts with the ether oxygen atoms of the phytyl chains, and the ring E carbomethoxy groups of each PC B850 (Freer *et al*., 1996). Reconstitution experiments in the LH1 system show that if the ring E carbomethoxy group is modified the formation of LH1 is suppressed (Parkes-Loach *et al*., 1990).

The glucoside head group of the carotenoid molecule in LH2 is the only part of this molecule capable of making specific interactions. This sugar moiety is found to be disordered in the LH2 structure, possibly taking up a dual conformation *via* rotation about the linker oxygen-sugar bond. The specificity of the carotenoid for the *Rps acidophila* 10050 LH2 is therefore thought to reside in the extent of conjugation present, and the concomitant steric consequences on the structure of the carotenoid itself. Table 6 gives protein contacts for this chromophore. A second, external carotenoid has been defined for each PC. However this is a poorly defined partial structure, and the conformation of the conjugated double bond system may not be defined from the electron density.

All remaining protein pigment interactions appear to be of a van der Waals character. Tables 3 to 6 list the contacts of the chromophores (only the closest approach residue atom to pigment atom)

Table 6. Apoprotein contacts to the rhodopin glucoside chromophore

Rhodopin glucoside atom	Residue	Atom	Distance (Å)
C4	Ile (−)α6	CA	3.81
	Lys (−)α5	O	3.78
	Val (−)α9	CG2	3.70
CM3	Tyr β14	CD2	3.43
C6	Leu β11	CD2	4.10
CM4	Gln (−)α3	OE1	3.54
C12	Val β15	O	3.87
C13	Leu α20	CD2	3.82
CM3	Gly β18	O	3.66
C14	Thr β19	OG1	3.37
C15	Phe β22	CB	4.26
C18	Val α23	CG2	3.64
C25	Ile α26	CG2	3.73
CM8	Ala (+)α27	CB	4.06
	Ile (+)α28	CG1	4.02
C27	His (+)α31	NE2	4.11

The carotenoid numbering scheme used is that outlined by Freer *et al*. (1996).

Table 7. Closest approach of bacteriochlorins and carotenoids

Pigment atom	Pigment atom	Distance (Å)
$\alpha B850\ C13^2$	$\beta B850\ O13^1$	3.36
$\alpha B850\ O17^3$	(−)Rhodopin CM8	3.59
$\alpha B850\ C2^1$	(−)βB850 C20	3.57
βB850 OP	Rhodopin C19	3.42
$B800\ O17^3$	Rhodopin CM6	3.42

for each independent pigment in turn. The closest approach between chromophores are listed in Table 7.

Site energy

In an organic solvent such as acetone, monomeric Bchl *a* absorbs at a wavelength of 777 nm (Weigl, 1953). Calculations based upon inter-pigment geometry in the LH2 complex (Sauer *et al*., 1996) cannot account fully for the difference in resonant absorptions arising from B800 and B850 pigments. Local environment effects modify this idealised system and must be considered for a complete analysis of the function of the molecule. A secondary role of the protein component of LH2 is to provide this local environment for each of the pigment moieties, such that the absorption properties of these molecules make efficient use of the light energy available to the bacterium.

Coordination effects

Bchl *a* is a porphyrin-type molecule with an asymmetric conjugated double-bond system resulting in two characteristic absorptions in the visible and infra red, arising from characteristic transition dipoles (Q_x and Q_y, respectively; van Grondelle *et al*., 1994). The transition dipoles of Bchl *a* lie within the plane of the bacteriochlorin system and any distortion of the molecule affects the absorption properties of the conjugated double-bond system (Barkiga *et al*., 1988). The distortion modes of porphyrin-like molecules generally arise from the coordination of an axial ligand and peripheral contacts to the molecule (Scheidt & Lee, 1987). As summarised earlier, specific contacts to all three independent Bchl *a* molecules in LH2 are made to the same groups on the bacteriochlorin system.

The Mg^{2+} central ion is penta-coordinated in all cases, but for B800 the ligating species contacts the Mg^{2+} from the opposite face of the bacteriochlorin system when compared to both B850 molecules. The structural consequences of this difference are slight, even though the bacteriochlorin system is chiral and a slightly different distortion mode may occur. A comparison of the αB850 bacteriochlorin and the B800 bacteriochlorin reveals that the ''opposing'' ligands produce little relative distortion of the pigments (Figure 4). The αB850 molecule is almost planar, the B800 molecule is slightly domed.

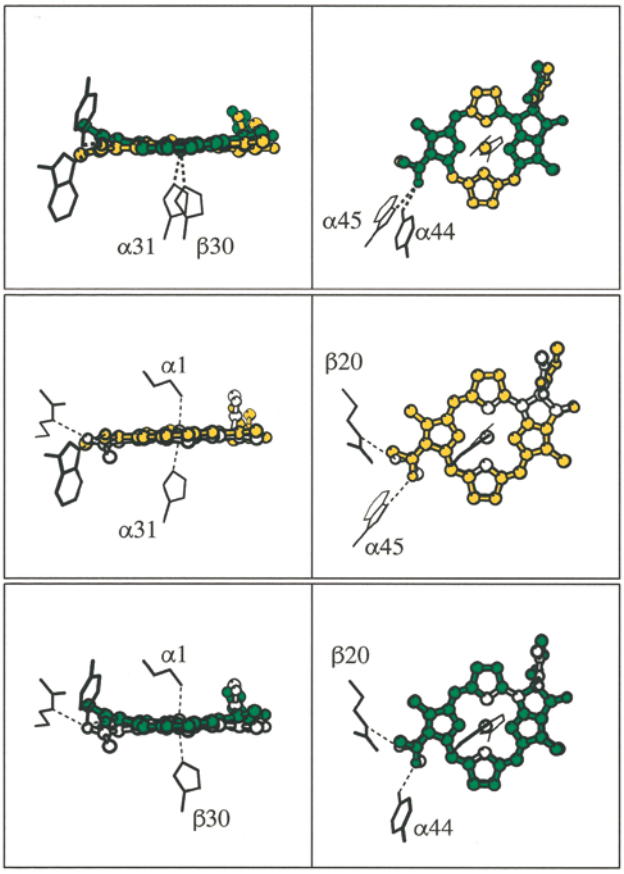

Figure 4. Overlay of PC bacteriochlorophylls and their contacts: Plan and elevation views. Overlays were generated by superimposing the core nitrogen atoms plus a carbon atom to define chirality (rms deviations were of the order 0.03 Å, program LSQKAB (CCP4, 1994)). αB850, yellow; βB850, green; B800, white; for clarity, peripheral groups on rings B and D have been removed, along with the phytyl chains (MOLSCRIPT; Kraulis, 1991).

The βB850 molecule is significantly distorted with respect to αB850 and B800 (Figure 4). The βB850 is in a saddle conformation with a significant bowing along the long axis of the conjugated double-bond system (coincident with the Q_y transition dipole). This molecular axis is terminated by the ring A acetyl group, which in βB850 accepts a hydrogen bond from αTyr44. This specific interaction is associated with a molecular distortion of the Bchl *a*, and, as the molecules absorbing at 850 nm form a delocalised system in terms of their excited properties, the consequences of this distortion will be manifest as a property of the LH2 complex itself (van Grondelle *et al.*, 1994). Calculations suggest that these distortions can lead to absorption red-shifts to the order of 100 nm in extreme cases (Barkigia *et al.*, 1988).

Additionally the disposition of the acetyl group, effectively the torsion angle about the C3-C3^1 bond, profoundly affects the absorption wavelength. Blue shifts of about 20 nm in Q_x and Q_y are calculated to occur if this torsion angle takes up values of ±90° (Hanson *et al.*, 1987). For B850 molecules the acetyl group is effectively co-planar with the bacteriochlorin system, and for B800 this torsion is within 30° of co-planarity. However a comparison of the acetyl disposition in B800 and B850 shows that the group is in an opposing orientation in B800 with respect to that of B850 (the torsion angle C2-C3-C3^1-O3^1 is 194/159° for α/βB850 and −30° in B800). This structural change between B800 and B850 means effectively that the two pigments differ as the symmetry of the chromophore differs.

As well as the structural consequences of protein pigment contacts (such as doming etc.), the local perturbation of the chromophore due to an interaction will result in a change in spectroscopic properties. The effect of the coordination of Mg^{2+} by a formyl oxygen atom in Bchl *a* has not been characterised. However the exchange of an imidazole ligand for a water molecule is calculated to produce blueshifts in Q_x and Q_y of the order of 10 and 3 nm, respectively (Hanson *et al.*, 1987). The formation of hydrogen bonds to the C3 acetyl and C13^1 keto groups of Bchl *a* will affect the absorption properties of the chromophore. At the absorption wavelengths of LH2 red shifts of around 3 and 6 nm for Q_x and Q_y are calculated to result from the C3 acetyl group accepting a hydrogen bond, and corresponding blueshifts occur should the C13^1 keto group accept a hydrogen bond (Hanson *et al.*, 1987). In LH2, all of the C3 acetyl groups of Bchl *a* accept a hydrogen bond, whilst none of the C13^1 keto groups does.

The effect of polar species

Molecular orbital calculations have indicated the effects of placing point charges close to the chromophore of Bchl *a* (Eccles & Hong, 1983; Hanson *et al.*, 1987). These studies show that point charges placed at a distance of 3.5 Å from rings A and C of the bacteriochlorin system are calculated to produce Q_y absorption shifts of the order of ±100 nm depending on the position (above or below the plane) and polarity of the charge. No such point charge is encountered in the LH2 structure in contact with either of these rings for any of the Bchl *a* molecules. The absorption shifts are not caused by point charges *per se* but rather the electric fields emanating from them, so any charge distributions in the locality of Bchl *a* molecules must be considered.

One obvious dipole is the ion pair close to the B800 site at β17/20. The two charges are however considerably removed from the centroid of the nearest ring, A (at 11/7 Å), and the net electric field is not perpendicular to the plane of ring A as in the optimal point charge orientation (Hanson *et al.*, 1987).

In the core of Bchl *a* the charge on the central magnesium ion is compensated by the coordinating nitrogen atoms of the bacteriochlorin. The sys-

tem has no overall net charge. However one can expect variations in the local values of charge over the core (Mg^{2+}, 4N) and the fifth ligand. In the B850 macrocycle, each B850 molecule is in close contact with two adjacent bacteriochlorins. Within a PC, rings C and E from each bacteriochlorin overlap each other, between PCs the overlap is between ring A from adjacent bacteriochlorins. For each B850 Bchl *a* the histidine residue coordinating the promoter mate abuts ring C. The geometry of B850 coordination means that ring C of all B850 molecules exists in a complex electrical field. Considering the large absorption shift calculated in the point charge simulations by Hanson *et al*. (1987) and that all B850s would experience the same field, a significant spectral shift may be induced.

The absorption properties of carotenoids are a function of the polarizability of the medium in which they are found (Andersson *et al*., 1991). The all-*trans* conjugated double-bond system of the wholly defined carotenoid is extensively immersed amongst bacteriochlorophylls. The limited number of protein interactions are with uncharged residues and within the conjugated stretch only two polar residues (αHis31 and αGln3) are in contact with the molecule (Table 6). The putative second independent carotenoid does not interact with polar residues over its defined region.

Mechanical effects

An inter-molecule van der Waals interaction energy may be factored out from general quantum mechanical expressions for transition energies in coupled chromophores (Kasha *et al*., 1965). The effects of the remaining van der Waals contacts to the chromophores should be considered. The mechanical forces applied to each pigment in the LH2 complex are in equilibrium with those exerted by the pigment itself. This will also result in a van der Waals interaction term. This complex effect is difficult to parameterise, and difficult to distinguish from the effects of distortions induced by coordination (doming, etc.). Contacts of chromphores with like chromophores, unlike chromophores, protein and the non-photoactive portions of pigment molecules all occur in LH2. The effects arising from these interactions are observable. The bandwidths of the Q_y Bchl *a* absorptions of LH2 are dependent on the detergent in which the complex is encapsulated. This is especially noticeable in LH2 complexes absorbing at 800 and 820 nm when the higher near IR absorption peak, is a function of the detergent used. This is thought to be due to the exposure of these pigments to the micelle encapsulating the complex. The most pronounced effect is seen in the structure and properties of the carotenoid molecules. In solution, all-*trans* carotenoid molecules have no circular dichroism signals (Frank & Cogdell, 1993) due to the symmetry of their chromophores. In LH2, the chromophore of the wholly defined carotenoid takes up a helical conformation, which imparts chirality to the conjugated double-bond system. A CD signal is observed for the carotenoid in LH2 (Frank & Cogdell, 1993) and this property is entirely due to steric interactions in the complex. The ramifications of the helical conformation of the carotenoid in LH2 include the possibility of energy state mixing (Koyama *et al*., 1996), which has been postulated to be integral to the energy transfer properties of these molecules (Nagae *et al*., 1993).

Net B800/850 difference

The splitting of the Q_y absorption band in the exciton-coupled array of B850 goes some way to explaining the absorption differences for B800 and B850 pigments. The manner in which the Q_y absorption of B850 molecules is further red-shifted with respect to B800 is a major question. The calculations by Sauer *et al*. (1996) indicate a site energy difference between B800 and B850 that corresponds to a red-shift of 19 nm for the 850 nm Q_y absorption. The absorption spectrum of the LH2 complex shows that the Q_x bands of the monomeric B800 Bchl *a* molecules, and the coupled array of B850 molecules overlay. This indicates that differences that specifically affect the relative Q_y absorptions should be considered in this regard.

If the effects of coordination (individually those giving rise to distortions, and local effects in the chromophore due to ligation), polar species and of mechanical interactions are considered independent to a first approximation, the following conclusions may be drawn. The coordination/ligation contacts of all Bchl *a*s are similar. However, the B800 molecule is coordinated through the opposite bacteriochlorin face, and has a flipped C3 acetyl group with respect to both B850s. Also the distortion modes of the bacteriochlorins are different. The distortion found in the βB850 molecule is the most pronounced, and by inference to the other B850, this conformational change cannot be correlated to Mg^{2+} coordination. It appears that a combination of mechanical effects and the peripheral C3 acetyl hydrogen bond has caused the two B850s to take up different conformations. Another possibility for a site energy difference arises from the effects of coordination and overlapping in the B850 ring, resulting in local electric field distributions. The distortion differences in B850 are greatest along the axis between ring A and C, the putative charge distribution variation occurs in the vicinity of ring C, and the C3 acetyl group is on ring A. This molecular axis is coincident with the Q_y transition dipole. The detailed analysis of the effects indicated here are however beyond the scope of this paper.

Spectral modulation

The studies by Hunter and co-workers (Fowler *et al*., 1992) have demonstrated the influence of the protein in LH2. These studies have shown that mutations of residues in the *Rb. sphaeroides* LH2, corre-

Table 8. Refinement of LH2

	Constrained (1 × PC)	Restrained (3 × PC)
Resolution limits (Å)	12.0–2.5	12.0–2.5
No. independent non-Hydrogen atoms[a]	988	3078
No. reflections $F > 2\sigma(F)$	27,855	27,855
R_{cryst} (%)	22.73	20.98
R_{free} (%)	25.32	24.65
Rms deviation from target geometry	0.019 Å; 2.129°	0.019 Å; 2.043°
Mean *B*-factor (Å^2)	34.52	38.97
Rms deviation on PC superimposition (Å)	–	0.060 (PC1-PC2), 0.053 (PC1-PC3)
Coordinate precision (Å)[b]	0.07	0.10
Estimated rms accuracy (Å)[c]	0.40	0.38

Unit cell: $a = b = 120.3$, $c = 296.2$ Å (hexagonal index). Spacegroup *R*32.

Anisotropic scaling correction (Å^2) applied to F_{obs}: $U_{11} = -0.0550$, $U_{22} = -0.0550$, $U_{33} = 0.1099$, $u_{12} = -0.1718$, $U_{13} = 0.0000$, $U_{23} = 0.0000$.

[a] In the initial report (McDermott *et al.*, 1995) hydrogen atoms used by X-PLOR were included in the number of independent atoms reported.

[b] Calculated with the expression for coordinate precision of atoms with low *B*-factors by D. W. J. Cruickshank (Dodson *et al.*, 1996). The geometrical and non-crystallographic symmetry restraints were included as observed parameters in the calculation. The high non-protein volume of the LH2 unit cell (73%) leads to an artificially low value for this figure.

[c] From the CCP4 (1994) program SIGMAA (Read, 1986).

sponding to those forming a hydrogen bond to the B850 C3 acetyl group in this structure, lead to absorption shifts in the 850 nm Q_y band (mutation Y44,Y45 to F44,Y45; 800 and 839 nm absorbing complex, mutation Y44,Y45 to F44,L45; 800 and 820 nm absorbing complex). Further studies (Hunter *et al.*, 1993) have indicated that the spectral shift is mainly due to the removal of a hydrogen bond rather than any π-π orbital interaction between B850 and an aromatic side-chain, and resonance Raman studies indicate the disruption of hydrogen bonding to the C3 acetyl groups (Fowler *et al.*, 1994). The absence of the ligand to the C3 acetyl group is calculated to affect both Q_x and Q_y with a magnitude of less than one half of the blue-shift encountered. Similarly, a change in the disposition of the C3 acetyl group cannot account for the blue-shifts as both transition dipoles are affected, and no significant shift or broadening in the Q_x absorption was reported. A movement in the relative dispositions of the B850 chromophores was not evident from CD measurements, therefore a change in either the oligomeric state of the LH2, or the coupling of the B850s is discounted. The mutations were conservative and did not change the net charge in the locality of the chromophores. The remaining influences of chromophore distortion and mechanical effects are likely candidates for modulating the spectra. However, without specific structural data the interpretation of these mutants cannot be complete.

Methods

The crystal structure of LH2 from *Rps. acidophila* strain 10050 was determined as described (McDermott *et al.*, 1995). The crystal structure shows a nonameric complex where subunits are arranged around an axis of 9-fold rotational symmetry (C_9). The model described in the initial report was refined further with the imposition of non-crystallographic symmetry using the program X-PLOR (Brunger, 1992b). Initially the non-crystallographic symmetry of the complex was constrained, and the model refined to convergence, as judged by the R_{free} (Brunger, 1992a). The C_9 equivalence was then heavily restrained (with a weight an order of magnitude higher than that applied to bond lengths). The flexibility of the restrained refinement protocol allowed crystal contacts and water structure to be released from precise equivalence. The quality of the current model and the data to parameter ratio (summarised in Table 8) indicate a reliable structure. The protein is 73% helical, and this large

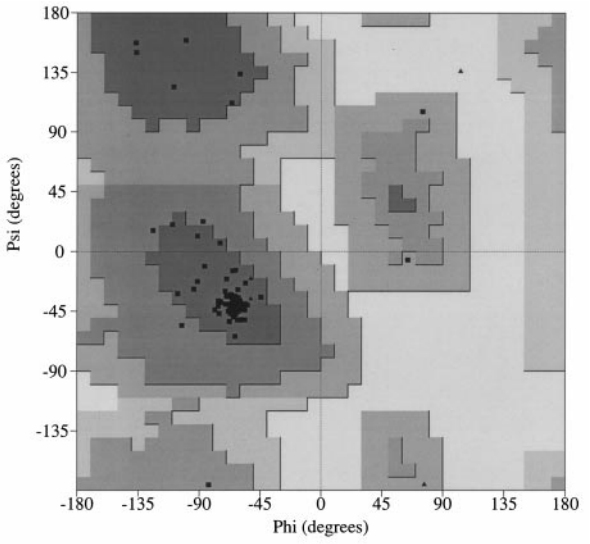

Figure 5. A Ramachandran (Ramachandran & Sasisekharan 1968) plot of the PC apoproteins (PROCHECK; Laskowski *et al.*, 1993).

proportion of regular structure leads to main chain stereochemistry reminiscent of a much higher resolution study (see the Ramachandran plot in Figure 5). A second carotenoid, which was reported in the initial structure (McDermott *et al*., 1995) as a detergent molecule (β-octyl-glucoside) has been assigned (Freer *et al*., 1996).

Crystallographic model

The membrane-spanning portion of LH2 consists of concentric cylinders of trans-membrane helices with the α apoproteins inner and β outer (Figure 1). The volume within the cylinder of α apoprotein helices is thought to contain lipid. A protomer complex (PC) may be defined as the unique portion of the complex, and the operation of the C_9 molecular symmetry axis upon the PC leads to the construction of the complete complex. The definition of the PC is arbitrary, as different considerations such as closest set of unique pigments, or most closely associated apoprotein heterodimer, lead to different PCs. Here, the PC is defined in terms of a radially associated αβ pair, i.e. the PC apoprotein pair lie on the same radius, which is perpendicular to the C_9 axis and passes through an α apoprotein trans-membrane helix then a β apoprotein trans-membrane helix. The PC is completed with those pigments most intimately associated with this heterodimer i.e. the Bchl *a* ligated to α or β and the most closely associated carotenoids (see Figure 1). The coordinates of the LH2 PC have been deposited at the Brookhaven Data Bank with accession number 1KZU.

The crystal structure of LH2 is subject to a different environment from that of the complex *in vivo*. LH2 is isolated from the native membrane by detergent solubilisation. From this point on the complex is partially encapsulated in a detergent micelle (Garavito *et al*., 1986). However, as LH2 may be assayed by absorption spectroscopy at any point in the purification process, and the spectrum of the protein pigment complex is very sensitive to structural change, we can be confident that the structure of LH2 is very similar to that found *in vivo*. At no point during the preparation of LH2 crystals is the complex disassembled. LH2 crystals are type II membrane protein crystals, where crystal contacts are formed only between hydrophilic parts of the protein (Michel, 1983). This means that the trans-membrane portions of LH2 are in no way compromised by the crystallization process *per se*.

An analysis of the atomic model of LH2 with programs VOIDOO and FLOOD (Kleywegt & Jones, 1994) has revealed apparent voids, close to the 800 nm absorbing Bchl *a* (B800) sites of the complex. An explanation for this is that the final sections of phytyl chains of the α-as-

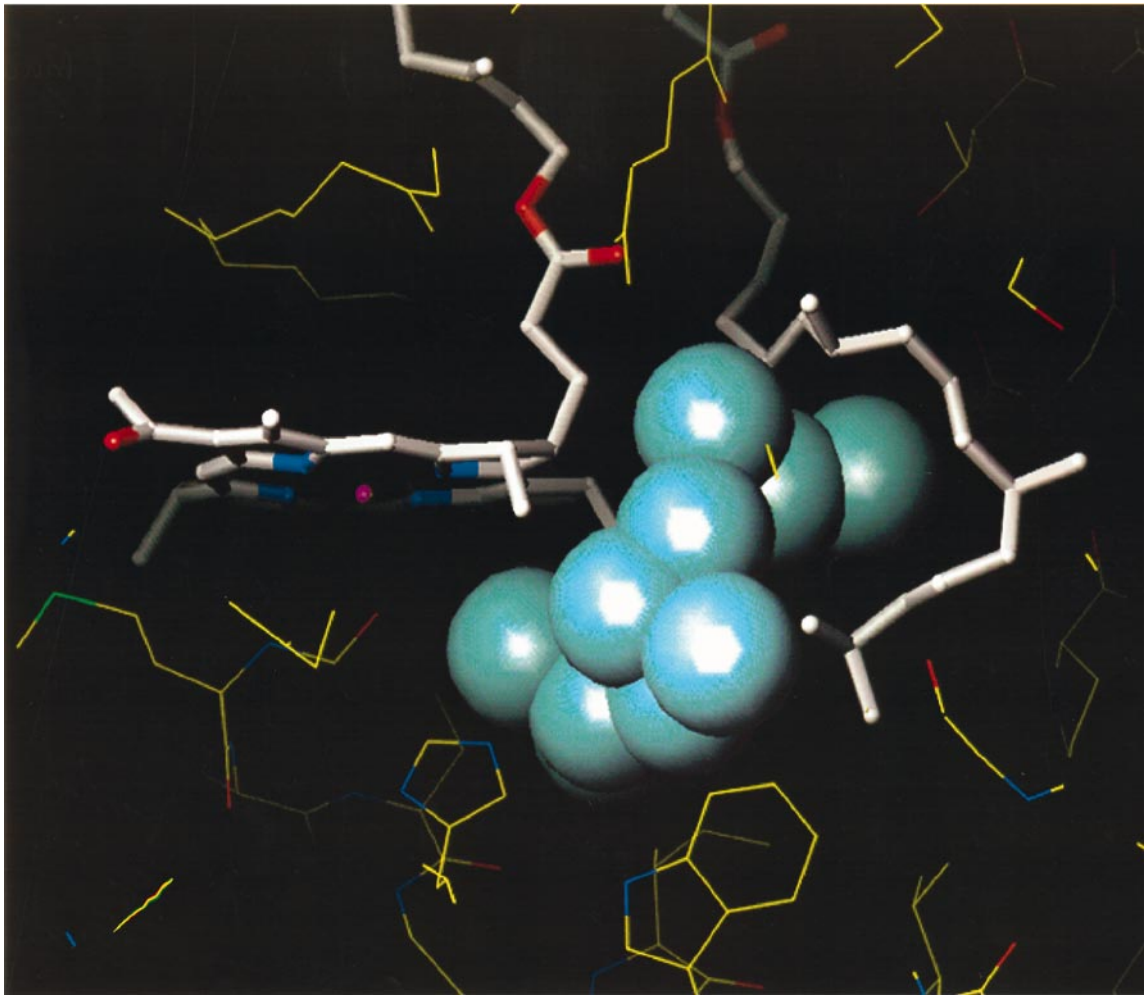

Figure 6. The grey van der Waals spheres show the likely repositioning of the αB850 phytyl chain. The B800 Bchl *a* and the phytyl chain of the αB850 are highlighted as thick bonds, the remaining protein is represented in thinner bonds (O; Jones *et al*., 1991).

sociated 850 nm absorbing Bchl *a* (αB850) molecules appear to have relaxed back towards the central lipid-filled portion of the structure (Figure 6). The space vacated has been filled by a water molecule (McDermott *et al*., 1995), plus relaxation of the surrounding protein. On solubilisation of the LH2 complex the environment within and without the toroidal structure is different from that *in vivo*; especially if detergent gains access to the central portion. This may account for the small reorientation of the αB850 phytyl chain, though no change in the relative disposition of the optically active portions of the light-harvesting pigments has been detected. The external carotenoid shows disorder, which may be induced by contact of the micelle.

Acknowledgements

We thank Professor Kenneth Sauer of the University of California, Berkeley, for instructive discussions. This work has been supported by the BBSRC Membrane Initiative.

References

Andersson, P. A., Gillbro, T., Ferguson, L. & Cogdell, R. J. (1991). Absorption spectral shifts of carotenoids related to medium polarizability. *Photochem. Photobiol.* **54**, 353–360.

Barkigia, K. M., Chantranupong, L., Smith, K. M. & Fajer, J. (1988). Structural and theoretical models of photosynthetic chromophores. Implications for redox, light absorption properties and vectorial electron flow. *J. Am. Chem. Soc.* **110**, 7566–7567.

Brunger, A. T. (1992a). Free *R* value a novel statistical quantity for assessing the accuracy of crystal structures. *Nature,* **355**, 472–475.

Brunger, A. T. (1992b). In *X-PLOR Version 3.1 A system for X-ray crystallography and NMR.* Yale University Press, New Haven & London.

Collaborative Computational Project, Number 4 (1994). The CCP4 suite: programs for protein crystallography. *Acta Crystallog. sect. D,* **50**, 760–763.

Cowan, S. W. (1993). Bacterial porins: lessons from three high-resolution structures. *Curr. Opin. Struct. Biol.* **3**, 501–507.

Dodson, E., Kleywegt, G. J. & Wilson, K. (1996). Report of a workshop on the use of statistical validators in protein X-ray crystallography. *Acta Crystallog. sect. D,* **52**, 228–234.

Eccles, J. & Hong, B. (1983). Charged amino acids as spectroscopic determinants for chlorophyll *in vivo*. *Proc. Natl Acad. Sci. USA,* **80**, 4959–4962.

Feher, G., Allen, J. P., Okamura, M. Y. & Rees, D. C. (1989). Structure and function of bacterial photosynthetic reaction centres. *Nature,* **339**, 111–116.

Fowler, G. J. S., Visschers, R. W., Greif, G. G., van Grondelle, R. & Hunter, C. N. (1992). Genetically modified photosynthetic antenna complexes with blueshifted absorbance bands. *Nature,* **355**, 848–850.

Fowler, G. J. S., Sockalingnum, G. D., Robert, B. & Hunter, C. N. (1994). Blue shifts in bacteriochlorophyll absorbance correlate with changed hydrogen bonding patterns in light-harvesting 2 mutants of *Rhodobacter sphaeroides* with alterations at α-Tyr-44 and α-Tyr-45. *Biochem. J.* **299**, 695–700.

Frank, H. A. & Cogdell, R. J. (1993). Photochemistry and function of carotenoids in photosynthesis. In *Carotenoids in Photosynthesis* (Young, A. & Britton, G., eds), pp. 252–326, Chapman & Hall, London.

Freer, A., Prince, S., Sauer, K., Papiz, M., Hawthornthwaite-Lawless, A., McDermott, G., Cogdell, R. & Isaacs, N. W. (1996). Pigment-pigment interactions and energy transfer in the antenna complex of the photosynthetic bacterium *Rps. acidophila*. *Structure,* **4**, 449–462.

Garavito, R. M., Markovic-Housley, Z. & Jenkins, J. A. (1986). The growth and characterisation of membrane protein crystals. *J. Cryst. Growth,* **76**, 701–709.

Hanson, L. K., Thompson, M. A. & Fajer, J. (1987). Environmental effects on the properties of chlorophylls *in vivo*. Theoretical models. In *Progress in Photosynthesis Research* (Biggins, J., ed.), pp. 311–314, Martinus Nihoff, Dordrecht.

Hawthornthwaite, A. M. & Cogdell, R. J. (1991). Bacteriochlorophyll-binding proteins. In *The Chlorophylls* (Scheer, H., ed.), pp. 493–528, CRC, Boca Raton, FL.

Hunter, C. N., Fowler, G. J. S., Greif, G. G. & Olsen, J. D. (1993). Protein engineering of bacterial light harvesting complexes. *Biochem. Soc. Trans.* **21**, 41–43.

Jirsakova, V., Ranck, J. L. & Reiss-Husson, F. (1995). Oligomeric states of the LHI and LHII complexes from *Rubrivax gelatinosus* in detergent solutions. In *Photosynthesis: from Light to Biosphere* (Mathias, P., ed.), vol. 1, pp. 219–222, Kluwer Academic Publishers, Dordrecht.

Jones, T. A., Zou, Z. Y., Cowan, S. W. & Kjeldgaard, M. (1991). Improved methods for building protein models in electron density maps and the location of errors in these models. *Acta. Crystallog. sect. A,* **47**, 110–119.

Karrasch, S., Bullough, P. A. & Ghosh, R. (1995). The 8.5 Å projection map of the light-harvesting complex I from *Rhodospirillum rubrum* reveals a ring composed of 16 subunits. *EMBO J.* **14**, 631–638.

Kasha, M., Rawls, H. R. & Ashraf El-Bayoumi, M. (1965). The exciton model in molecular spectroscopy. *Pure Appl. Chem.* **11**, 371–392.

Kleywegt, G. J. & Jones, T. A. (1994). Detection, delineation measurement and display of cavities in macromolecular structures. *Acta. Crystallog. sect. D,* **50**, 178–185.

Koepke, J., Hu, X., Muenke, C., Schulten, K. & Michel, H. (1996). The crystal structure of the light-harvesting complex II (B800-850) from *Rhodospirillum molischianum*. *Structure,* **4**, 581–597.

Koyama, Y., Kuki, M., Andersson, P. O. & Gillbro, T. (1996). Singlet excited states and the light-harvesting function of carotenoids in bacterial photosynthesis. *Photochem. Photobiol.* **63**, 243–256.

Kraulis, P. J. (1991). MOLSCRIPT: a program to produce both detailed and schematic plots of protein structures. *J. Appl. Crystallog.* **24**, 946–950.

Kuhlbrandt, W. (1995). Structure and function of bacterial light-harvesting complexes. *Structure,* **3**, 521–525.

Laskowski, R. A., MacArthur, M. W., Moss, D. S. & Thornton, J. M. (1993). A program to check the stereochemical quality of protein structures. *J. Appl. Crystallog.* **26**, 283–291.

McDermott, G., Prince, S. M., Freer, A. A., Hawthornthwaite-Lawless, A. M., Papiz, M. Z., Cogdell, R. J. & Isaacs, N. W. (1995). Crystal structure of an integral membrane light-harvesting

complex from photosynthetic bacteria. *Nature,* **374**, 517–521.
Michel, H. (1983). Crystallization of membrane proteins. *Trends Biochem. Sci.* **8**, 56–59.
Nagae, H., Kakitani, T., Katoh, T. & Mimuro, M. (1993). Calculation of the excitation transfer matrix elements between the S_2 or S_1 state of bacteriochlorophyll. *J. Chem. Phys.* **98**, 8012–8023.
Parkes-Loach, P. S., Michalski, T. J., Bass, W. J., Smith, U. & Loach, P. A. (1990). Probing the bacteriochlorophyll binding site by reconstitution of the light harvesting complex of *Rhodospirillum rubrum* with bacteriochlorophyll *a* analogues. *Biochemistry,* **29**, 2951–2960.
Papiz, M. Z., Prince, S. M., Hawthornthwaite-Lawless, A. M., McDermott, G., Freer, A., Isaacs, N. W. & Cogdell, R. J. (1996). A model for the photosynthetic apparatus of purple bacteria. *Trends Plant Sci.* **1**, 198–206.
Ramachandran, G. N. & Sasisekharan, V. (1968). Conformation of polypeptides and proteins. In *Advances in Protein Chemistry* (Anfinsen, J. B., Anson, M. L., Edsall, J. T. & Richards, F. M., eds), vol. 23, pp. 283–438, Academic Press, New York and London.
Read, R. J. (1986). Improved Fourier coefficients for maps using phases from partial structures with errors. *Acta Crystallog. sect. A,* **42**, 140–149.
Robert, B. & Lutz, M. (1985). Structure of antenna complexes of several *Rhodospirillales* from their resonance Raman spectra. *Biochim. Biophys. Acta,* **807**, 10–23.
Sauer, K., Cogdell, R. J., Prince, S. M., Freer, A., Isaacs, N. W. & Scheer, H. (1996). Structure-based calculations of the optical spectra of the LH2 bacteriochlorophyll protein complex from *Rhodopseudomonas acidophila*. *Photochem. Photobiol.* **64**, 564–576.
Savage, H., Cyrklaff, M., Monotoya, G., Kuhlbrandt, W. & Sinning, I. (1996). Two-dimensional structure of light harvesting complex II (LH II) from the purple bacterium *Rhodovulum sulpidophilum* and comparison with LH II from *Rhodopseudomonas acidophila*. *Structure,* **4**, 243–252.
Scheer, H. (1991). Structure and occurrence of chlorophylls. In *The Chlorophylls* (Scheer, H., ed.), pp. 3–30, CRC, Boca Raton, FL.
Scheidt, W. R. & Lee, Y. J. (1987). Recent advances in the stereochemistry of metallotetrapyrroles. In *Structure and Bonding* (Buchler, J. W., ed.), vol. 64, pp. 1–70, Springer-Verlag, Berlin.
van Grondelle, R. V., Dekker, J. P., Gillbro, T. & Sundstrom, V. (1994). Energy transfer and trapping in photosynthesis. *Biochim. Biophys. Acta,* **1187**, 1–65.
Weigl, J. W. (1953). Concerning the absorption spectrum of bacteriochlorophyll. *J. Am. Chem. Soc.* **75**, 999–1000.
Zuber, H. (1986). Structure of light-harvesting antenna complexes of photosynthetic bacteria, cyanobacteria and red algae. *Trends Biochem. Sci.* **11**, 414–419.
Zuber, H. & Brunisholz, R. A. (1991). Structure and function of antenna polypeptides and chlorophyll-protein complexes: principles and variability. In *The Chlorophylls* (Scheer, H., ed.), pp. 627–703, CRC, Boca Raton, FL.

Edited by R. Huber

(Received 4 July 1996; received in revised form 3 February 1997; accepted 3 February 1997)